Earthquake-based passive seismic exploration techniques

Polychronopoulou, K.; Lois, A.; Martakis, N.; Calassou, S.; Draganov, D.

DOI
10.1190/segam2019-w21-04.1

Publication date
2019

Document Version
Accepted author manuscript

Published in
SEG Technical Program Expanded Abstracts 2019

Citation (APA)
Polychronopoulou, K., Lois, A., Martakis, N., Calassou, S., & Draganov, D. (2019). Earthquake-based passive seismic exploration techniques. In *SEG Technical Program Expanded Abstracts 2019* (pp. 5393-5397). Society of Exploration Geophysicists. https://doi.org/10.1190/segam2019-w21-04.1

Earthquake-based passive seismic exploration techniques

K. Polychronopoulou (Seismotech S.A.), A. Lois (Seismotech S.A.), N. Martakis (Seismotech S.A.), S. Calassou (TOTAL E&P/R&D), and D. Draganov (TU Delft)*

Summary

Passive seismic surveys have long been applied in the context of exploration studies. Our research focuses on the exploitation of the natural seismicity that is present in passive seismic records and the extraction of useful information of the subsurface from different parts of the earthquake signal. In that scope, we initially install a dense seismological network in an area of interest that will permit the recording of local microseismicity and we detect and locate microearthquakes of very small magnitude that occur within a very close distance from this network. We then exploit the isolated earthquake signals, applying different passive seismic techniques, in order to extract the different pieces of information that they are carrying. More specifically, we use their P- and S-wave first arrivals to perform local earthquake tomography, acquiring a tomographic P- and S-wave velocity distribution of the subsurface below the area of interest. We also extract their P- and S-wave coda to perform reflected-wave seismic interferometry by autocorrelation, which provides zero-offset virtual reflection responses from virtual sources sending energy nearly vertically down below each station of the installed network. The acquired results, which are both individually interpreted and jointly evaluated, provide a valuable insight on the subsurface.

Introduction

Passive seismic is a term incorporating a broad range of techniques that aim to illuminate the subsurface exploiting the natural or man-made signals that exist in continuous passive seismic records, without the implication of any controlled sources (e.g., Verdon *et al.,* 2010; de Ridder *et al.*, 2011; Boullenger *et al.*, 2015). We focus on the exploitation of local microearthquakes of very small magnitude that naturally occur in an area of interest as passive seismic sources.

The main advantage of using earthquake-based passive seismic techniques is that the sources are characterized by known properties, such as their occurrence time and hypocentral location, or even their focal characteristics. Microearthquake signals include different types of waves, carrying diverse pieces of information about the medium. These waves can be isolated and exploited by different passive seismic techniques in order to extract interesting information. On the other hand, being dependent on the natural microseismicity of an area involves being exposed to two uncontrollable factors: the microearthquakes' spatial distribution and occurrence rate. These factors, which can be predicted for an area, but with a large degree of uncertainty, have a significant impact on the acquired results, especially in areas where seismicity is marginal or non-uniformly distributed.

The dataset

In order to apply any earthquake-based passive seismic technique, we initially have to acquire a suitable passive dataset. Such dataset usually consists of continuous recordings from a number of stand-alone seismological stations, covering an area of interest, with interstation distances that depend on the target size and depth. The type of sensors that are installed mainly depends on the intended passive seismic technique, since the frequency band of interest largely varies in relation to an earthquake's magnitude. For exploration-scale applications, we exploit relatively high-frequency local microearthquakes of very small magnitude, thus we do not need to use broadband sensors. A network of three-component short-period stations, or even geophone nodes, is adequate to record the useful signals. The duration of the recording period is highly dependent on the seismicity of the area under investigation.

Location of the microearthquake sources

The first processing step we apply is the accurate location of local microseismicity. With the term microseismicity, we refer to local earthquakes of very small magnitude (< 2 R) that occur within a very close distance (< 5 km) from an area of interest. These microearthquakes, which occur in abundance at the majority of the earth's locations, are usually not recorded by global or regional seismological networks. Thus, we must accurately detect and locate them in, often, months-lasting continuous passive seismic records.

In order to do this, we perform automatic seismological analysis of the acquired dataset. This analysis consists of two stages. We initially detect "candidate events", applying an energy-based algorithm (Leontarakis *et al.*, 2015), using information from all three components of the recorded signals. The detected events are then isolated from the continuous records and a "clean-up" procedure, based on multi-station analysis, is applied, in order to minimize the number of false alarms. Then, we automatically estimate the P- and S-waves' onset times of the thus-selected events, exploiting the statistical characteristics of the detected signals (Lois *et al.*, 2013). The estimated P- and S-wave arrival times are then used to calculate hypocentral locations of the detected events, resulting in a catalogue of the local microearthquakes that occurred during the recording period.

An example of a passive seismic network is depicted in Figure 1. This network was installed in SW France, in the context of the MAUPASACQ project (Chevrot *et al.*, 2018). It consists of 440 stations (53 broadband, 197 short-period stations and 190 geophone nodes), covering an area of approximately 1500 km^2. The short-period stations are installed on a regular grid of 3x3 km, while the geophone nodes densify specific lines, with an inter-station distance of 1 km. The broadband stations are either co-located with other stations inside the network or installed around it, serving as peripheral stations in the scope of ensuring a better hypocentral control of the recorded seismicity. The MAUPASACQ passive seismic network was continuously recording for a period of 6 months (April to September 2017). During this period, 1847 microseismic events were located within or around the study area (Figure 1).

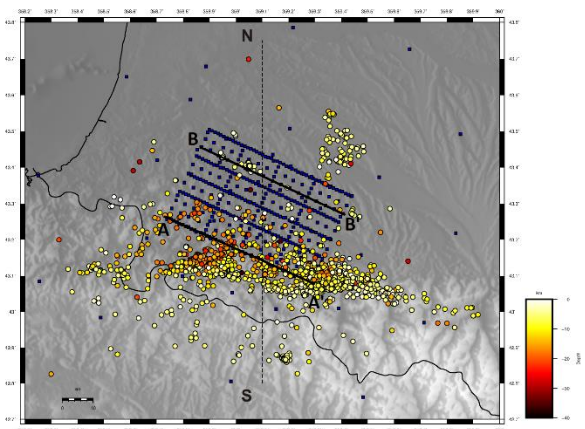

Figure 1: Seismicity recorded by the MAUPASACQ network during the six-month recording period. Blue rectangles correspond to the 440 recording stations, while the colour-coded circles depict the located microearthquakes. The colour scale corresponds to the events' hypocentral depths.

The different types of instruments of the MAUPASACQ network provide the opportunity to evaluate each instrument's adequacy for specific applications (Polychronopoulou *et al.*, 2018), while the seismicity's uneven spatial distribution permits evaluating the effect of irregular coverage, in terms of seismic rays, on the applied earthquake-based passive seismic techniques.

Local Earthquake Tomography (LET)

The first arrivals of both the P- and S-waves of the recorded microearthquakes are used as input for LET. We perform a joint hypocenter – velocity inversion, using a revised version of the SIMULPS code (Evans *et al.*, 1994). We invert for both P- and S-wave velocity (V_p and V_s), while we relocate the recorded seismicity, using the updated velocity models, at each iteration. This procedure results in an estimation of the 3D V_p and V_p/V_s distributions below the study area. These tomographic models can be either individually interpreted, or used as input in the context of the application of other passive seismic techniques (e.g., time-to-depth conversion of seismic interferometry (SI) virtual reflection responses).

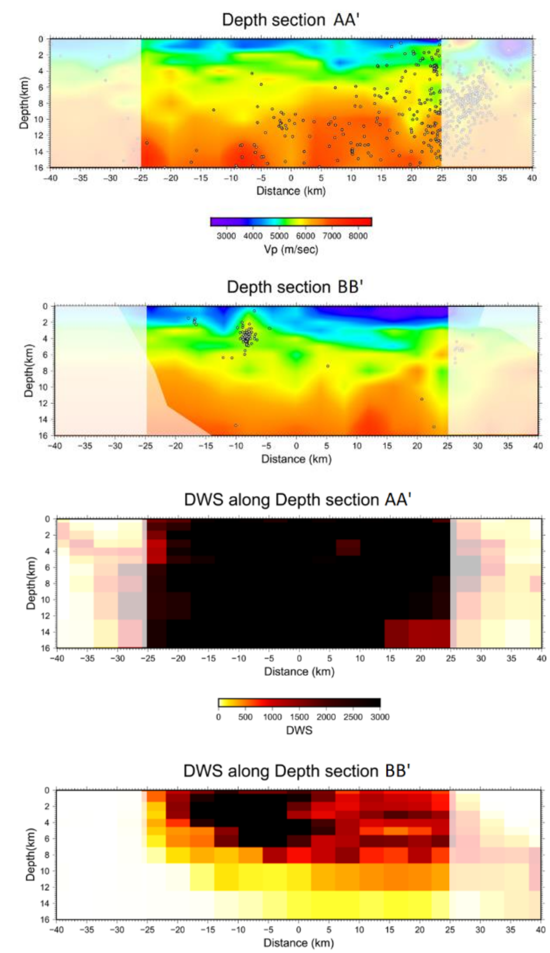

Figure 2: LET results along the cross-sections AA' and BB' of Figure 1. Top two panels: Vp distribution from mean sea level, down to a depth of 16 km. Dots correspond to hypocentral locations of events, which occurred at a maximum distance of 5 km towards each side of the cross-section, projected on each line. Bottom two panels: Derivative weighted sum distribution along the same lines.

In the case of the MAUPASACQ dataset, we apply LET using the estimated 209105 P- and S-wave arrival times (114361 P-wave and 94744 S-wave onset times) of 1847 located microearthquakes. We parameterize the model space using a 4x4x1-km grid along the x, y, and z axis, respectively. The inverted volume extends from the surface down to a depth of 20 km. An example of the obtained results is presented in Figure 2. It consists of the V_p distribution calculated by LET along cross-sections AA' and BB' of Figure 1. The Vp models are accompanied by the relevant distribution of the Derivative Weighted Sum (DWS), which is indicative of the quality of the solution at each area of the model space. DWS is calculated by summing all the ray segments inside the region of influence of each model parameter, after weighting them according to their distance from the parameter itself. Observing Figure 2, it becomes evident that, despite the large number of first arrivals that were used for the tomography, their irregular distribution and the consequent inhomogeneous coverage of the study area, in terms of seismic rays, resulted in a model characterized by variable uncertainty.

Reflected-wave Passive Seismic Interferometry (SI)

From the located microearthquakes whose first P- and S-wave arrivals are nearly vertical at each of the recording stations, we extract the P- and S-wave coda and then use them as input signals for the application of reflected-wave SI by autocorrelation (Wapenaar *et al.*, 2010). By this, we calculate stacked autocorrelograms (per component) below each station, using the signals of the events passing the verticality criterion for this particular station, after applying spiking deconvolution on the original signals, in the scope of enhancing their vertical resolution. These stacked autocorrelation functions of the deconvolved signals correspond to zero-offset reflection responses below each station that would be produced by a virtual source co-located with the station and emitting energy nearly vertically down. We then process the retrieved zero-offset virtual reflection responses, using conventional seismic-exploration processing techniques.

The spatial distribution of the microearthquakes located in the context of the MAUPASACQ project did not permit the recording of adequate input signal for all the installed stations, thus underlining a limitation of using SI by autocorrelation on nearly vertical signals. The verticality criterion significantly reduced the number of exploitable microearthquakes, resulting in the calculation of robust virtual reflection responses below only 223 of the 440 stations. However, the results acquired at the stations where adequate signal was available provide very valuable information of the subsurface, showing the methodology's potential as an exploration tool. In Figure 3, a depth section of the virtual reflection responses along the cross-section AA' of Figure 1 is presented. Time-to-depth conversion is performed using an average 1D velocity model calculated from the resulting model from LET.

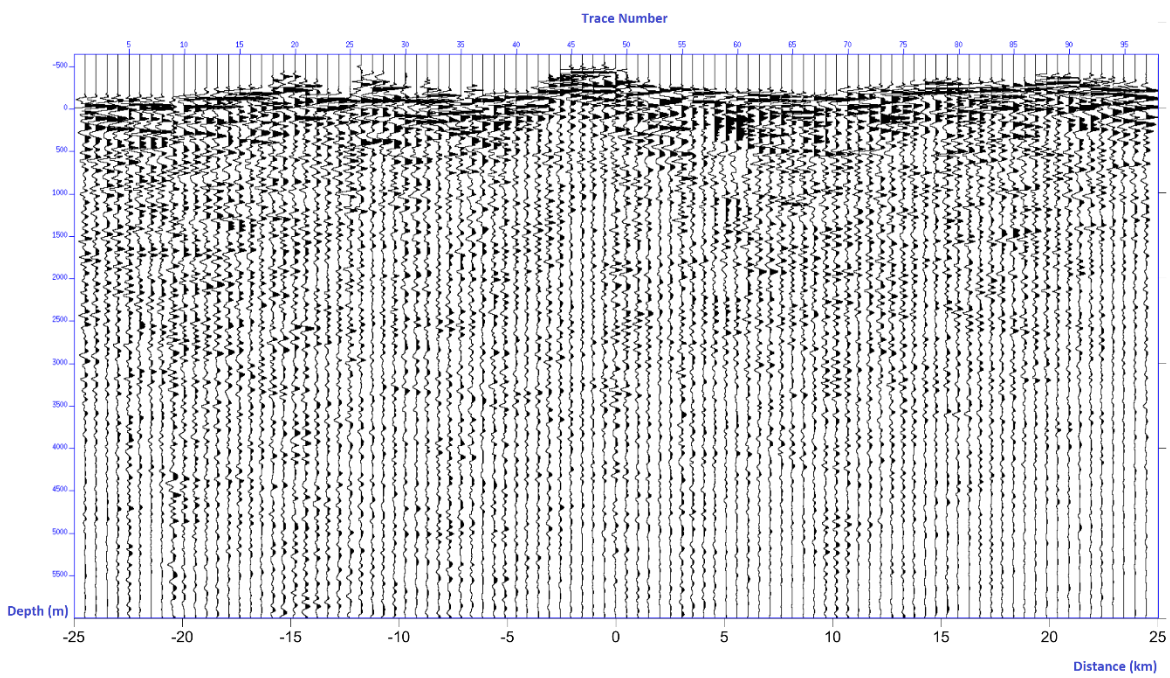

Figure 3: Depth section of the virtual reflection responses along the cross-section AA' of Figure 1, from the surface down to a depth of 6 km.

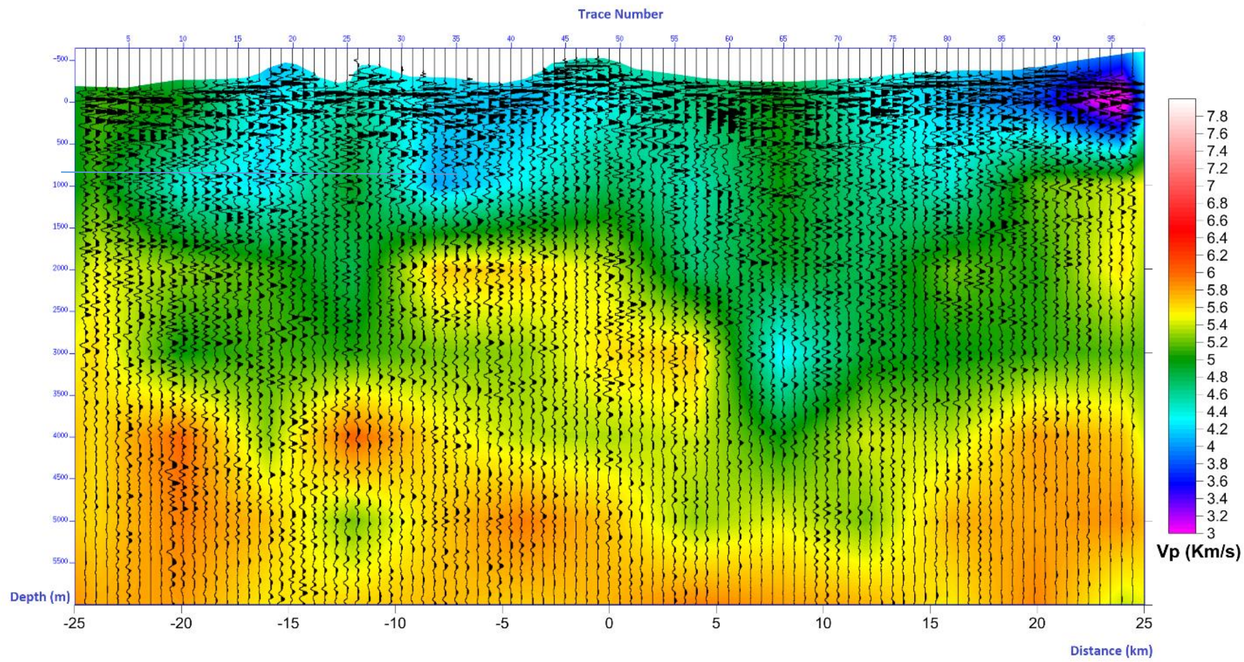

Figure 4: The depth section of Figure 3 superimposed on the corresponding LET V_p distribution.

The virtual reflectors are also superimposed on the V_p distribution of Figure 2, along the same line (Figure 4), showing the existence of coherent information in the output of both passive seismic techniques. Even though a thorough interpretation of the acquired results is beyond the scope of the present work, it is important to note some of the remarks deriving from their joint evaluation. Observing Figure 4, it becomes evident that, even though the vertical resolution of the output of SI and LET are not comparable and the virtual reflectors provide a much more detailed image of the subsurface, especially at the shallower parts of the cross-section, the major features are present in both results. Apart from the many structures appearing on the velocity distribution that are also delineated by SI-retrieved reflectors, there are also parts of the depth section, where the reflectivity seems to be "weakened" in comparison to neighboring traces. These parts (e.g., see Figure 4 around traces 35, 65, and 75 at the depth of 800, 3000, and 600 m, respectively) coincide with lower-velocity zones of the LET model with relatively steep boundaries. Such steep boundaries will not result in retrieved reflections from virtual sources emitting energy nearly vertically down.

We apply SI by autocorrelation to part of the MAUPASACQ network, due to the imposed verticality criterion. To the rest of the stations, we plan to apply SI by crosscorrelation to the P- and S-wave coda taking the mutual orientation of the stations and the microearthquakes into account (Nishitsuji *et al.*, 2016)

Conclusions

Earthquake-based passive seismic techniques show a great potential as exploration tools. The detection and location of local microearthquakes in a continuous passive seismic record provides a dataset of passive sources, characterized by known location and occurrence time. These sources can be exploited using a number of different techniques, aiming in revealing the information that exists hidden in the different types of waves that constitute the earthquake signal. Even though earthquake-based passive seismic methodologies may suffer from their dependence on the existence of exploitable seismicity in an area of interest, they can provide valuable information on the subsurface from the very near-surface down to depths of more than 10 km. Application of local earthquake tomography and reflected-wave passive seismic interferometry on the MAUPASACQ dataset shows that, even in the unfavorable cases where the seismicity is unevenly distributed, it is possible to acquire a robust image of the subsurface in the parts of the study area where there is adequate earthquake signal.

Acknowledgements

The MAUPASACQ passive seismic acquisition has been realized by collaboration of TOTAL E&P/R&D, CNRS, BRGM, Seismotech S.A. and CSIC-Barcelona, in the context of the OROGEN project, funded by TOTAL S.A., CNRS and BRGM.

References

Boullenger, B., A. Verdel, B. Paap, J. Thorbecke, and D. Draganov, 2015, Studying CO2-storage with ambient-noise seismic interferometry: a combined numerical feasibility study and field-data example for Ketzin, Germany: Geophysics, **80**(1), Q1-Q13, doi: 10.1190/geo2014-0181.1.

Chevrot, S., M. Sylvander, J. Diaz, A. Villasenor, N. Martakis, K Polychronopoulou, P. L'Excellent, M. Collin, E. Masini, S. Calassou, S. Beller, R. Martin, L. Stehly, P. Boue, B. Bouin and A. Bitri, 2018, The large-N and large-T MAUPASACQ experiment – A very dense seismic network to image the deep architecture of the western Pyrenees: Geophysical Research Abstracts, **20**, EGU2018-11926.

De Ridder, S. and J. Dellinger, 2011, Ambient seismic noise eikonal tomography for near-surface imaging at Valhall: The Leading Edge, **30**(5), 506-512.

Evans, J. R., D. Eberhart-Phillips, and C. H. Thurber, 1994, User's Manual for SIMULPS12 for Imaging vp and vp/vs: A derivative of the "Thurber" tomographic inversion SIMUL3 for Local Earthquakes and Explosions: Open-file Report 94-431, U.S. Geological Survey. 101 pp.

Leontarakis, K., A. Lois, A. Pantazopoulos, and K. Polychronopoulou, 2015, A comprehensive methodology for automated analysis of seismic records and its contribution to a Passive Seismic Tomography survey in Delvina, SW Albania: SEG 85th Annual Meeting, Expanded Abstracts, 2563-2567.

Lois, A., E. Sokos, N. Martakis, K. Paraskevopoulos, and G-A. Tselentis, 2013, A new automatic S-onset detection technique: Application in local earthquake data. Geophysics, **78**(1), KS1-KS11.

Nishitsuji, Y., S. Minato, B. Boullenger, M. Gòmez, K. Wapenaar, and D. Draganov, 2016, Crustal-scale reflection imaging and interpretation by passive seismic interferometry using local earthquakes: Interpretation, **4**, SJ29-SJ53, doi:10.1190/INT-2015-0226.1.

Polychronopoulou, K., A. Lois, N. Martakis, S. Chevrot, M. Sylvander, J. Diaz, A. Villasenor, S. Calassou, M. Collin, E. Masini, A. Bitri and L. Stehly, 2018, Broad-band, short-period or geophone nodes? Quality assessment of passive seismic signals acquired during the MAUPASACQ experiment: First Break, **36**(4), 71-76.

Verdon, J. P., J-M. Kendall, D. J. White, D. A. Angus, Q. J. Fisher, and T. Urbancic, 2010, Passive seismic monitoring of carbon dioxide storage at Weyburn: The Leading Edge, **29**(2), 200-206.

Wapenaar K., D. Draganov, R. Snieder, X. Campman, and A. Verdel, 2010, Tutorial on seismic interferometry: Part1 – Basic principles and applications: Geophysics **75**(5), 75A195–75A209.